第 31 卷第 9 期
2015 年 9 月

无 机 化 学 学 报
CHINESE JOURNAL OF INORGANIC CHEMISTRY

Vol.31 No.9
1831-1838

基于多齿希夫碱配体的四核和十核锰簇合物的合成、结构和磁性

杨晓迅　冷际东　刘俊良　贾建华*　童明良

(中山大学化学与化学工程学院,生物无机与合成化学教育部重点实验室,广州　510275)

摘要：合成了一种具有{NO_4}给电子组成的多齿水杨醛希夫碱配体,3,5-二-叔丁基水杨醛-三(羟甲基)氨基甲烷(H_4L),并利用元素分析、红外光谱以及核磁共振氢谱表征其结构。$Mn(ClO_4)_2$ 或 $MnCl_2\cdot 4H_2O$ 分别与该配体在溶液中反应生成了一个四核锰簇合物$[Mn^{III}_4(HL)_2(H_2L)_2(MeCN)_4](ClO_4)_2\cdot 2MeCN$ (**1**)和一个十核锰簇合物$[Mn^{III}_6Mn^{II}_4(bz)_{10}(L)_4(H_2O)_2]\cdot 10MeCN$ (**2**)。X-射线衍射分析表明化合物 **1** 的晶体结构空间群为三斜 $P\bar{1}$,而化合物 **2** 为正交 *Aba*2。2~300 K 温度区间的磁性测量数据表明化合物 **2** 中存在反铁磁相互作用。

关键词：希夫碱；锰簇合物；反铁磁相互作用

中图分类号：O614.71+1　　**文献标识码**：A　　**文章编号**：1001-4861(2015)09-1831-08

DOI:10.11862/CJIC.2015.260

Synthesis, Structures and Magnetic Properties of Two Tetranuclear and Decanuclear Manganese Clusters Bearing the Multidentate Schiff-Base Ligands

YANG Xiao-Xun　LENG Ji-Dong　LIU Jun-Liang　JIA Jian-Hua*　TONG Ming-Liang

(*MOE Key Laboratory of Bioinorganic and Synthetic Chemistry, School of Chemistry and Chemical Engineering, Sun Yat-Sen University, Guangzhou* 510275, *China*)

Abstract: A multidentate salicylaldehyde Schiff-base ligand with {NO_4} donor set, 3,5-di-tert-butylsalicylaldehyde-trihydroxymethylaminomethane (H_4L), has been synthesized for the first time and characterized by elemental analysis, IR and ^{1}H NMR. Solution reactions of $Mn(ClO_4)_2$ or $MnCl_2\cdot 4H_2O$ with H_4L in air generated a tetranuclear complex $[Mn^{III}_4(HL)_2(H_2L)_2(MeCN)_4](ClO_4)_2\cdot 2MeCN$ (**1**) and a decanuclear complex $[Mn^{III}_6Mn^{II}_4(bz)_{10}(L)_4(H_2O)_2]\cdot 10MeCN$ (**2**), respectively. X-ray studies reveal that complex **1** crystallizes in triclinic space group $P\bar{1}$, while complex **2** crystallizes in orthorhombic space group *Aba*2. Magnetism data in the temperature range 2~300 K have been carried out, indicating the presence of the antiferromagnetic interaction within **2**.

Key words: Schiff-base; manganese cluster; antiferromagnetic interaction

In 1993, $Mn_{12}Ac$ as the first single -molecule magnet (SMM) that could retain magnetization in the absence of magnetic field was discovered [1-2]. This unexpected result has led to a great expansion in the investigation of the synthesis and magnetic property for polymetallic molecular species, especially those with large spin ground-state *S* and axial zero-field splitting parameter *D* values, which are widely accepted as the most important features as SMMs determination [3]. True to its name, the SMM is a molecule that behaves as an individual nanomagnet. Because of their small size and precise

收稿日期:2015-05-29。收修改稿日期:2015-07-13。

国家重点基础研究发展规划("973 计划", No.2014CB845602,2012CB821704),国家自然科学基金(No.21301197,91122032,21371183,91422302),广东省自然科学基金(S2013020013002),以及中央高校基本科研业务费专项资金(14lgpy10)资助项目。

*通讯联系人。E-mail:jiajh3@mail.sysu.edu.cn

characterization, SMMs straddle the classical and quantum mechanical worlds, displaying many interesting features and having important technological applications in fields of information storage and quantum computation, etc [4]. Complexes involving manganese ions have held a very important seat in SMMs family, up to now, particularly the Mn_{12} and Mn_6 clusters [5-6]. Generally speaking, the spin value can be successfully maximized when ferromagnetic-coupling systems are generating [7]. One important direction to reach this goal is developing the new synthetic procedure for polynuclear clusters, among which the design of key ligands is extremely promising. In this regard, hydroxyl-rich ligands as well as acid ligands [8-14], such as tripodal alcohols, have been widely used for the development of polynuclear molecular species.

Recent years, multidentate hydroxyl-rich Schiff-base ligands have attracted much attention due to their significantly potential applications in site selection, catalysis, biochemistry and magnetochemistry. They have been identified as highly effective ligands for the construction of polymetallic SMMs because of the similar coordination superiorities as hydroxyl-rich ligands[15-21]. For example, the tridentate Schiff-base ligand, 5-bromo-2-salicylideneamino-1-propanol ($H_2$5-Br-sap), has been used to construct dinuclear and tetranuclear SMMs previously [16,18].

Inspired by these precedents, we recently began to investigate a multidentate salicylaldehyde Schiff-base ligand 3,5-di-tert-butylsalicylaldehyde-trihydroxymethylaminomethane (H_4L) with $\{NO_4\}$ donor set, which may provide an effective direction for molecular magnets design. Fortunately, two novel manganese clusters $[Mn^{III}_4(HL)_2(H_2L)_2(MeCN)_4](ClO_4)_2 \cdot 2MeCN$ (**1**) and $[Mn^{III}_6Mn^{II}_4(bz)_{10}(L)_4(H_2O)_2] \cdot 10MeCN$ (**2**), were obtained from reactions of Mn(Ⅱ) salts with H_4L (Scheme 1). Herein, we reported their synthesis, structures and magnetic properties.

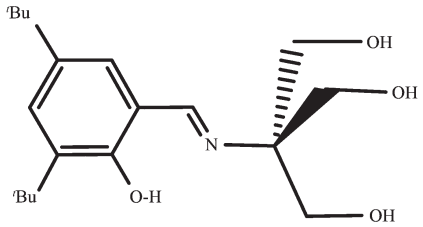

Scheme 1 Schiff-base ligand H_4L

1 Experimental Section

1.1 Physical measurements

Elemental analysis was performed on an Elementar Vario-EL CHNS elemental analyzer. IR spectra were recorded from KBr pellets in the range 4 000~400 cm^{-1} on a Bruker-EQUINOX 55 spectrometer. ^1H NMR spectra were recorded on a Mercury-Plus 300 nuclear magnetic resonance analyzer using TMS as internal standard. Variable-temperature magnetic susceptibility and magnetization measurements were performed with a Quantum Design MPMS-XL 7 SQUID. Dried powder samples were embedded in petroleum jelly to prevent torquing. Direct current (dc) susceptibility data were collected at zero dc field and were corrected with Pascal constants.

1.2 Synthesis

All materials were commercially available and used as received without further purification. All manipulations were performed under ambient laboratory conditions.

H_4L. To a methanol solution (100 mL), trihydroxymethylaminomethane (1.79 g, 15 mmol) was added with magnetic stirring. Then, 3,5-di-tert-butylsalicylaldehyde (3.52 g, 15 mmol) was added to the above solution slowly at 80 ℃ under reflux. The resulting solution turned yellow, and was continued to reflux for further 1 h. After removing the solvent by reduced pressure distillation, yellow powder with obvious scent was obtained (98.7% yield). IR data

(KBr, cm^{-1}): 3 473s, 3 356s, 2 962m, 2 360m, 1 617s, 1 477w, 1 365m, 1 203s, 1 049s, 875m, 850m, 831s, 727m, 649m, 572m. ^{1}H NMR data: δ 8.36 (1H); 7.36 (1H); 7.26 (1H); 4.90 (1H); 3.84 (6H); 1.92 (3H); 1.32 (18H). Anal. Calcd. for $C_{19}H_{31}NO_4$ (%): C, 67.63; H, 9.26; N, 4.15; Found (%): C, 67.65; H, 9.27; N, 4.17.

$[Mn^{III}_4(HL)_2(H_2L)_2(MeCN)_4](ClO_4)_2\cdot 2MeCN$ (**1**). To a solution of $Mn(ClO_4)_2$ (0.543 g, 1.5 mmol) in acetonitrile (15 mL), mixture solution of H_4L (0.169 g, 0.5 mmol) and ethanolamine (0.092 g, 1.5 mmol) in acetonitrile (10 mL) was added dropwise with magnetic stirring. A black solution was obtained and continued to stir for 7 h. After filtration, the filtrate was allowed to evaporate at room temperature. Ten days later, only a few red block crystals suitable for X-ray analysis were obtained along with massive black microcrystals (less than 2% yield).

$[Mn^{III}_6Mn^{II}_4(bz)_{10}(L)_4(H_2O)_2]\cdot 10MeCN$ (**2**). To a solution of $MnCl_2\cdot 4H_2O$ (0.059 g, 0.3 mmol) in methanol (15 mL), a solution of H_4L (0.034 g, 0.1 mmol) in acetonitrile (15 mL) was added dropwise with magnetic stirring. The resulting solution turned black. About half an hour, solid sodium benzoate (0.086 g, 0.6 mmol) was added, then the mixture was stirred at room temperature for 7 h and filtered. The filtrate with light reddish brown color was evaporated at room temperature. Three days later, red block crystals suitable for X-ray analysis were collected. (ca. 40% yield based on H_4L). IR data (KBr, cm^{-1}): 3 498m, 3 396m, 3 361w, 2 989m, 2 773m, 2 032s, 1 778w, 1 623s, 1 473m, 1 390w, 1 203m, 1 045w, 972w, 835m, 732m, 655w, 567m. Anal. Calcd. for $C_{166}H_{192}N_{14}O_{38}Mn_{10}$ (%): C, 56.31; H, 5.47; N, 5.54; Found (%): C, 56.28; H, 5.48; N, 5.56.

1.3 X-ray crystallography

Diffraction intensities of **1** and **2** were collected on a Bruker Smart Apex CCD diffractometer using graphite-monochromated Cu $K\alpha$ hradiation (λ=0.154 178 nm). Absorption corrections were processed through multiscan program SADABS [22]. The structures were

Table 1　Crystallographic Data and Structural Refinements for 1 and 2

Complex	**1**	**2**
Empirical formula	$C_{88}H_{132}N_{10}O_{24}Cl_2Mn_4$	$C_{166}H_{192}N_{14}O_{38}Mn_{10}$
Formula weight	2 004.70	3 540.74
Crystal system	Triclinic	Orthorhombic
Space group	$P\bar{1}$	*Aba2*
a / nm	1.203 03(6)	2.394 95(9)
b / nm	1.290 17(8)	2.078 37(6)
c / nm	1.773 80(9)	3.825 82(16)
α / (°)	104.669(5)	
β / (°)	107.856(4)	
γ / (°)	90.066(4)	
V / nm^3	2.525 8(2)	19.043 4(12)
Z	1	4
D_c / ($g\cdot cm^{-3}$)	1.318	1.235
T / K	123(2)	123(2)
GOF	0.988	1.020
Reflns collected	17 339	21 537
F(000)	1 056	7 360
R_{int}	0.039 3	0.061 3
Data / restrains / parameters	7 199/84/586	10 883/169/1 100
R_1[a], wR_2[b] ($I>2\sigma(I)$)	0.078 3, 0.215 6	0.074 1, 0.179 9
R_1[a], wR_2[b] (all data)	0.114 4, 0.235 2	0.112 5, 0.221 0

[a] $R_1=\Sigma \| F_o\|-|F_c\| / \Sigma |F_o|$, [b] $wR_2=[\Sigma w(F_o^2-F_c^2)^2/\Sigma w(F_o^2)^2]^{1/2}$

solved with direct method and refined with a full-matrix least-squares technique with the SHELXTL program package[23]. The hydrogen atoms were placed in idealised positions and refined using a riding model.

Data collection parameters and structure refinement details are listed in Table 1.

CCDC: 1403158, **1**; 1403159, **2**.

2 Results and discussion

2.1 Synthesis

The condensation reaction of trihydroxymethylaminomethane with 3,5-di-*tert*-butylsalicylaldehyde in methanol solution under reflux gave the target product H_4L in 98.7% yield (Scheme 2).

Solution reaction of $Mn(ClO_4)_2$ with H_4L in air can afford dark solution after seven hours. Evaporation of the resulting mixture at room temperature finally yielded crystals **1** in less than 2% yield. Crystals **2** were obtained in 40% yield from solution reaction of $MnCl_2$ with H_4L and sodium benzoate. Given that the starting manganese sources were exclusively Mn^{II} ions, it is apparent that Mn^{III} ions generated by oxidation of Mn^{II} ions, a common process in manganese cluster chemistry[24]. As an immediate color change of solution to black was observed during the reagents mixing for both preparation process of **1** and **2**, it is proposed that oxidation step occurs in the process of initial reaction rather than crystallization step. To our surprise, alcohol hydroxyls of H_4L in **1** are partly deprotonated in the presence of base, whereas for **2** alcohol hydroxyls are completely deprotonated without any base. Hence, the extent of deprotonation of the ligand exerts great influence on the buildings of metal clusters, especially high nuclearity metal clusters. Generally speaking, the more thoroughly the ligands are deprotonated, the higher nuclearity species would be obtained. In order to figure out the conditions for deprotonation of the ligand and the impact of metal salts, auxiliary ligands and solvents on the constructions of complexes with such Schiff-base ligand, many attempts have been done upon reaction system of **2**. Replacement of $MnCl_2$ by other manganese salts such as $Mn(OAc)_2$, $Mn(NO_3)_2$ and $Mn(ClO_4)_2$ in the same reaction condition only yielded amorphous powder. In addition, reactions under various solvent conditions were in vain. Due to the excellent property of N_3^- unit in magnetism transmission, moreover, NaN_3 was incorporated into the reaction system, unfortunately there is no any crystal obtained except some powder. So far, combination of $MnCl_2$, sodium benzoate, mixed solvents of methanol and acetonitrile, seems to be the best choice for reaction system to generate **2**.

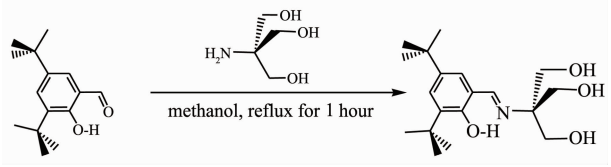

Scheme 2 Synthetic route of H_4L

2.2 Structure description

Single-crystal X-ray structural analysis reveals that the structure of **1** consists of four Mn^{III} ions (Fig. 1), crystallizing in triclinic space group $P\bar{1}$. Four alcohol hydroxyls in ligand H_4L are partly deprotonated while completely deprotonated in **2**. All four Mn^{III} ions in **1** are six-coordinated with near-octahedral geometry. Four coordination sites of each Mn^{III} ion in equatorial plane are occupied by phenoxyl oxygen atom, amine nitrogen atom, and two hydroxyl oxygen atoms from L^{4-}. The other two axial sites are occupied by two nitrogen atoms from two acetonitrile molecules for Mn1 and two hydroxyl oxygen atoms from two L^{4-} for Mn2, respectively (Fig.1).

The bond lengths of Mn1-O/N and Mn2-O/N are respectively in the range of 0.184 9(2)~0.195 5(3) nm, 0.185 3(3)~0.203 2(2) nm in the equatorial plane and 0.225 7(4)~0.234 6(4) nm, 0.213 6(2)~0.215 4(2) nm

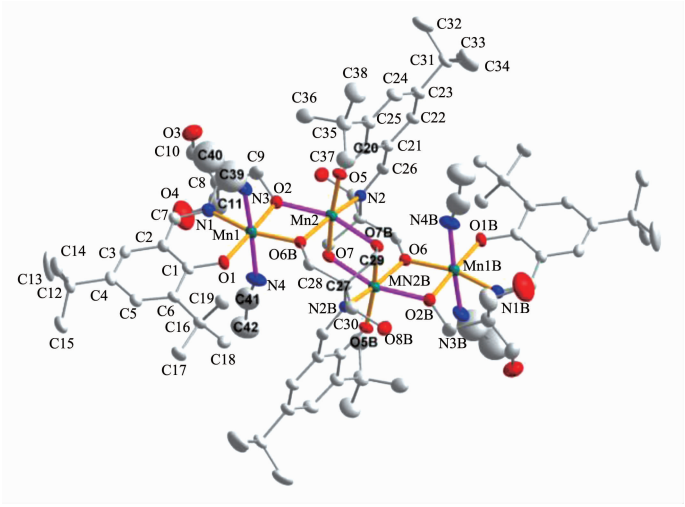

Thermal ellipsoids are displayed at the 30% probability level. Hydrogen atoms are omitted for clarity. Color code: Mn^{III}, teal; N, blue; O, red; C, gray; and the elongated Jahn-Teller axes of Mn^{III} ions are highlighted in pink. Symmetry code: B: 1−*x*, 1−*y*, 1−*z*

Fig.1　ORTEP diagram of **1**

in the axis, which indicates coordination geometry of Mn^{III} ions are elongated octahedron, displaying a Jahn-Teller distortion. Meanwhile the mean bond length of Mn1-N (0.229 9(7) nm, Jahn-Telle axis) is longer than that of Mn2-O (0.2144 (5) nm, Jahn-Telle axis). Similarly, the N3-Mn1-N4 angle of Jahn-Teller axis in Mn1 (173.2(3)°) is found a little bit larger than that of O2-Mn2-O7A in Mn2 (159.19(15)°). These comparisons indicate the octahedral configuration of Mn1 is more elongated than that of Mn2.

Complex **2** crystallizing in orthorhombic space group *Aba*2 consists of two linear pentanuclear $Mn^{II}_2Mn^{III}_3$ parts (Fig.2), which are further connected by oxygen atoms from L^{4-} and benzoate ions, forming a very beautiful cross-like $Mn^{II}_4Mn^{III}_6$ core (Fig.3). Three manganese ions (Mn1, Mn3, Mn5) of each pentanuclear $Mn^{II}_2Mn^{III}_3$ unit are found to be trivalent, the rest two manganese ions (Mn2, Mn4) are Mn^{II} ions. Mn^{III} and Mn^{II} ions are arranged alternately. All Mn^{III} ions (Mn1, Mn3, Mn5, and their symmetry-related counterparts) are five-coordinated with square-pyramid as coordination polyhedron as shown in Fig.4 ($MnNO_4$

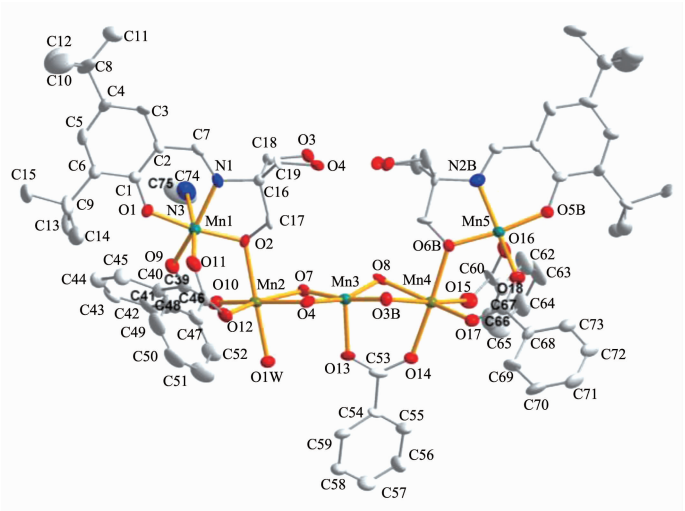

Thermal ellipsoids are displayed at the 30% probability level. Hydrogen atoms are omitted for clarity. Color code: Mn^{III}, teal; Mn^{II}, dark yellow; N, blue; O, red; C, gray. H atoms have been omitted for clarity. Symmetry code: B: 2−*x*, 1−*y*, *z*

Fig.2　ORTEP diagram of the linear pentanuclear part of **2**

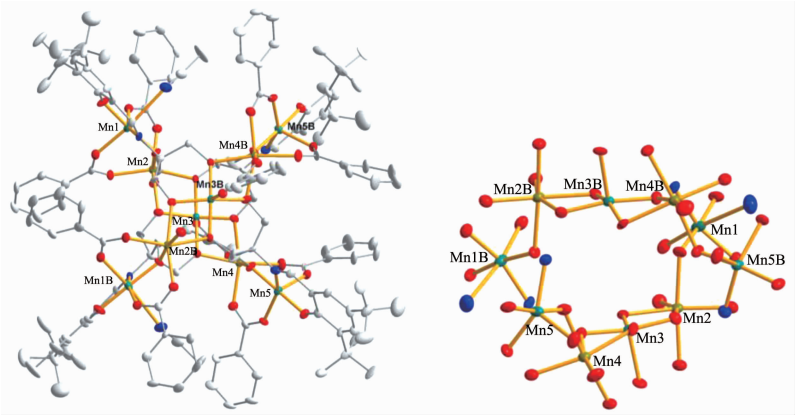

Thermal ellipsoids are displayed at the 30% probability level. Hydrogen atoms are omitted for clarity. Color code: Mn^{III}, teal; Mn^{II}, dark yellow; N, blue; O, red; C, gray. Symmetry code: B: 2–*x*, 1–*y*, *z*

Fig.3 ORTEP diagram of the independent molecule (left) and the $\{Mn^{II}_4Mn^{III}_6\}$ core (right) of **2**

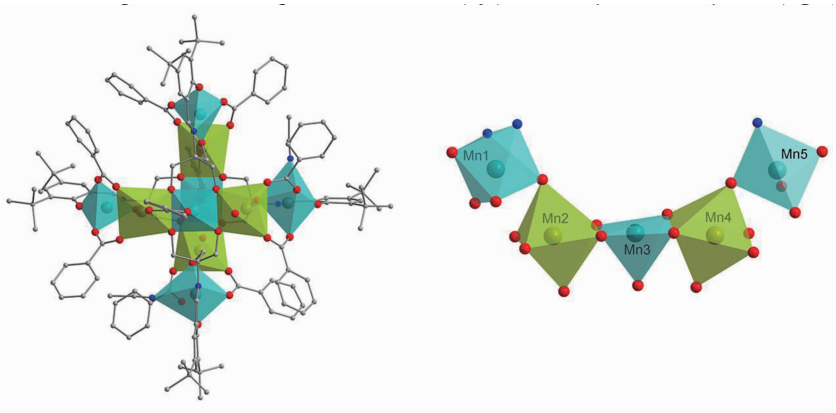

Thermal ellipsoids are displayed at the 30% probability level. Hydrogen atoms are omitted for clarity. Color code: Mn^{III}, teal; Mn^{II}, dark yellow; N, blue; O, red; C, gray

Fig.4 Polyhedral representation of molecule (left) and the linear pentanuclear part (right) of **2**

for Mn1 and Mn5, MnO_5 for Mn3). Four coordination sites in square are occupied by phenoxyl oxygen atom, amine nitrogen atom (or replaced by hydroxyl oxygen atom), hydroxyl oxygen atom, and oxygen atom of benzoate. The apical site is occupied by benzoate oxygen atom. The bond lengths of Mn^{III}-O/N are in the range of 0.184 9(8)~0.198 8(9) nm in the square and 0.210 9(7)~0.213 9(9) nm at the apex. In contrast to Mn^{III} ions, each Mn^{II} ion (Mn2, Mn4, and their symmetry-related counterparts) is surrounded by six oxygen atoms in octahedral geometry (MnO_6, Fig.4), which are respectively from hydroxyl groups of the L^{4-}, benzoate, and water molecule. Coordination bond lengths of Mn^{II}-O are in the range of 0.211 0(8)~0.221 8(7) nm and 0.211 8(9)~0.221 2(8) nm for Mn2 and Mn4, respectively.

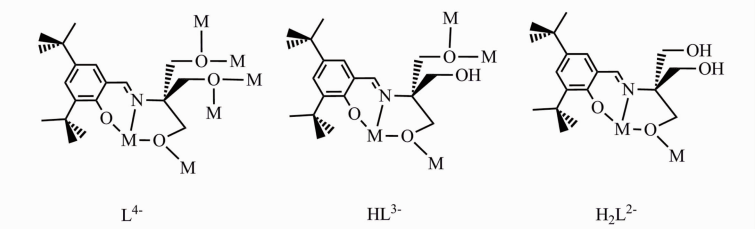

Scheme 3 Coordination modes of H_4L in **1** and **2**

Only weak intermolecular interactions are observed in both **1** and **2** involving that from benzene rings of ligands H_4L. The H_4L ligand displays the different coordination modes in **1** and **2** (Scheme 3), however, both act as chelating and bridging ligands.

2.3 Magnetic property study

Variable-temperature dc magnetic susceptibility data for **2** were collected in the temperature range 2~300 K, under an applied field of 1 000 Oe. The data plotted as $\chi_M T$ vs T in the Fig.5 are found to obey Curie-Weiss law $\chi(T)=C/(T-\theta)$ in the temperature range 60~300 K, giving the Curie constant C=42.17 $cm^3 \cdot mol^{-1} \cdot K$ and Curie-Weiss temperature θ=−93.08 K. Such large negative θ value indicates antiferromagnetic exchange interactions among manganese ions, and the high C value emphasizes the significant orbital contribution to the susceptibility. The room-temperature value of $\chi_M T$ is 32.14 $cm^3 \cdot mol^{-1} \cdot K$, smaller than the excepted spin-only value of 35.50 $cm^3 \cdot mol^{-1} \cdot K$ with $S_{Mn(II)}$=5/2, $S_{Mn(III)}$=2 and g=2 for a noninteracting $Mn^{II}_4Mn^{III}_6$ unit. Upon cooling, the $\chi_M T$ values gradually decrease to 5.16 $cm^3 \cdot mol^{-1} \cdot K$ at 2 K indicating an $S>0$ ground state. Fig.6 shows the isothermal magnetization in the field of 0~7 T at 2 K. The data also reveal the presence of the predominant antiferromagnetic interactions in **2**, which is consistent with the result obtained from magnetic susceptibility data.

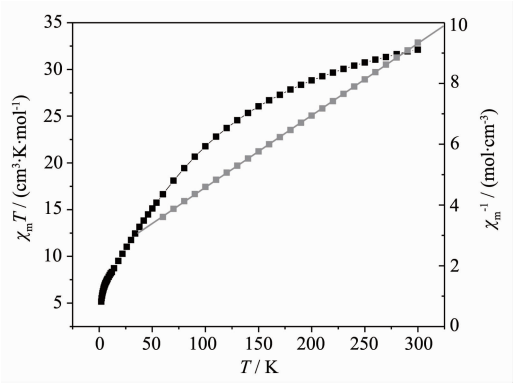

Fig.5　Plot of $\chi_M T$ versus T and plot χ_M^{-1} versus T at an applied field of 1 000 Oe for **2**

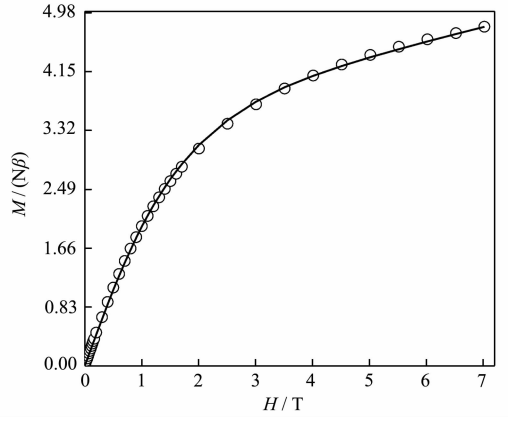

Solid line is guide for the eyes

Fig.6　Field dependence of magnetization at T=2.0 K

3 Conclusions

In this work, two novel manganese clusters with tetranuclear Mn^{III}_4 core and decanuclear cross-like $Mn^{II}_4Mn^{III}_6$ core surrounded by the new multidentate salicylaldehyde Schiff-base ligands H_4L with $\{NO_4\}$ donor set. Magnetic property studies reveal that antiferromagnetic exchange interactions occur in **2**, which may provide useful insights into magnetic exchange interactions in polynuclear manganese complexes. Moreover, the extent of deprotonation of H_4L ligands and the choice of proper auxiliary ligands are the key points in constructing high-nuclearity clusters with Schiff-base ligands.

References:

[1] Sessoli R, Tsai H L, Schake A R, et al. *J. Am. Chem. Soc.*, **1993**,**115**:1804-1816

[2] Sessoli R, Gatteschi D, Caneschi A, et al. *Nature*, **1993**,**365**:141-143

[3] Aromí G, Brechin E K. *Struct. Bond.*, **2006**,**122**:1-67

[4] Friedman J R, Sarachik M P. *Annu. Rev. Condens. Matter Phys.*, **2010**,**1**:109-128

[5] Gatteschi D, Sessoli R. *Angew. Chem. Int. Ed.*, **2003**,**42**:268-297

[6] Christou G, Gatteschi D, Hendrickson D N, et al. *MRS Bull.*, **2000**,**25**:66-71

[7] Ako A M, Hewitt I J, Mereacre V, et al. *Angew. Chem. Int. Ed.*, **2006**,**45**:4926-4929

[8] Manoli M, Prescimone A, Bagai R, et al. *Inorg. Chem.*, **2007**, **46**:6968-6979

[9] Moushi E E, Lampropoulos C, Wernsdorfer W, et al. *Inorg. Chem.*, **2007**,**46**:3795-3797

[10]Murugesu M, Raftery J, Wernsdorfer W, et al. *Inorg. Chem.*,

2004,**43**:4203-4209

[11]Rumberger E M, Shah S J, Beedle C C, et al. *Inorg. Chem*., **2005**,**44**:2742-2752

[12]YAO Hong-Chang(要红昌), WANG Ning(王宁), LI Miao-Miao(李淼淼), et al. *J. Zhengzhou Univ*.: *Nat. Sci. Ed*.(郑州大学学报:理学版), **2008**,**40**:88-94

[13]WANG Peng-Fei(汪鹏飞), WANG Xin(汪新), WU Guang-Hui(伍光辉), et al. *Chinese J. Inorg. Chem*.(无机化学学报), **2011**,**27**:1881-1886

[14]ZHOU Ai-Ju(周爱菊), LIANG Jing-Jing(梁晶晶), ZHENG Yan-Zhen(郑彦臻), et al. *Chinese J. Inorg. Chem*.(无机化学学报), **2012**,**28**:2425-2430

[15]Fontecha J B, Goetz S, McKee V. *Dalton Trans*., **2005**:923-929

[16]Oshio H, Hoshino N, Ito T, et al. *J. Am. Chem. Soc*., **2004**, **126**:8805-8812

[17]Oshio H, Hoshino N, Ito T, et al. *Angew. Chem. Int. Ed*., **2003**,**42**:223-225

[18]Oshio H, Nihei M, Yoshida A, et al. *Chem. Eur. J*., **2005**, **11**:843-848

[19]Oshio H, Nakano M. *Chem. Eur. J*., **2005**,**11**:5178-5185

[20]Bagai R, Abboud K A, Christou G. *Dalton Trans*., **2006**: 3306-3312

[21]Hoshiko J A, Wang G, Ziller J W, et al. *Dalton Trans*., **2008**:5712-5714

[22]Sheldrick G M. *SADABS*, University of Göttingen, Germany, **2002**.

[23]Sheldrick G M. *Acta Crystallogr*., **2008**,**A64**:112-122

[24]Hewitt I J, Tang J K, Madhu N T, et al. *Chem. Commun*., **2006**:2650-2652